# Neuroendocrine Transdifferentiation in Human Prostate Cancer Cells: An Integrated Approach

Marianna Cerasuolo[a,1], Debora Paris[b,1], Fabio A. Iannotti[b], Dominique Melck[b], Roberta Verde[b], Enrico Mazzarella[b], Andrea Motta[b] and Alessia Ligresti[b,2].

[a]University of Portsmouth, Department of Mathematics, Hampshire PO1 3HF, UK
[b]Endocannabinoid Research Group, Institute of Biomolecular Chemistry, Consiglio Nazionale delle Ricerche, 80078 Pozzuoli, Italy

[1]These authors equally contributed to this work

Running Title: Neuroendocrine Trans-differentiation in Human Prostate Cancer Cells

[2]To whom correspondence may be addressed
Alessia Ligresti, PhD
Institute of Biomolecular Chemistry
National Research Council of Italy
Via Campi Flegrei 34
80078 Pozzuoli (NA), Italy
Tel +39 081 867 5315
Fax +39 081 867 5340
e-mail: aligresti@icb.cnr.it

The authors declare no conflict of interest

**ABSTRACT** Prostate cancer (PCa) is highly sensitive to hormone therapy because androgens are essential for prostate cancer cell growth. However, with the nearly invariable progression of this disease to androgen independence (AI), endocrine therapy ultimately fails to control PCa in most patients. AI acquisition may involve neuroendocrine (NE) transdifferentiation, but there is little knowledge about this process, which is presently controversial. In this study, we investigated this question in a novel model of human androgen-dependent LNCaP cells cultured for long periods in hormone-deprived conditions. Strikingly, characterization of the NE phenotype by transcriptomic, metabolomic and other statistically integrated analyses showed how hormone-deprived LNCaP cells could transdifferentiate to a non-malignant NE phenotype. Notably, conditioned media from NE-like cells affected LNCaP cell proliferation. Predictive in silico models illustrated how after an initial period, when LNCaP cell survival was compromised by an arising population of NE-like cells, a sudden trend reversal occurred in which the NE-like cells functioned to sustain the remaining androgen-dependent LNCaP cells. Our findings provide direct biological and molecular support for the concept that NE transdifferentiation in PCa cell populations influences the progression to androgen independence.

**Major Findings:** Our integrated approach merging mathematical modeling with experimental data examines androgen-dependent PCa response to long-term/sustained hormone deprived conditions, and NE role in the progression to hormone refractory status. Using the tools of applied mathematics, we demonstrated that the non-malignant NE-phenotype, achievable under permanent androgen deprivation conditions, over time paradoxically contribute to the sustainment of undetectable androgen-dependent malignant cells.

**Keywords**: Prostate Cancer, LNCaP cells, Neuroendocrine Trans-differentiation, Integrated Omics, Mathematical Modeling

**Quick Guide to Equations and Assumptions:** Here we present a non-linear system of delay differential equations describing the interaction between malignant LNCaP and non-malignant trans-differentiated NE-like cell populations. The system in first approximation mimics experiments on cells growing in a Petri dish in androgen deprived conditions and builds mainly off previous works by Adimy et al. (1,2), adapting their model for cell cycle in hematopoiesis to our case. Furthermore, the model acknowledges previous works on prostate cancer development in single patients (3,4), where most of the models consider two populations of cancer cells: one population androgen dependent (AD), and the other population androgen independent (AI) (3). These studies describe *in vivo* conditions, and both AD and AI cells are able to proliferate. In our model we also consider two cell populations, one androgen sensitive (LNCaP), and the other androgen insensitive (NE-like), with sizes at time $t$ represented by $L(t)$ and $N(t)$ respectively. We assume that NE-like cells are post-mitotic and are produced through trans-differentiation by the first population. In addition, we consider that LNCaP cells go through asymmetrical cell division generating both undifferentiated and differentiated daughter cells. Finally, the model describes the dynamics of androgen concentration by referring to the percentage of charcoal stripped serum introduced in the medium ($A(t)$). As the serum was the only exogenous source of androgen in the experiments, and as there is a direct proportionality between serum and androgen content, from now on we refer in an equivalent way to charcoal stripped serum and androgen levels. The following system represents the dynamics of the three introduced quantities:

$$\underbrace{\frac{dA(t)}{dt}}_{\text{Androgen}} = \underbrace{-\varphi A(t)}_{A\text{ depletion}} + \underbrace{\kappa N(t)}_{\text{feedback from } NE \text{ to } A} \qquad (A.1)$$

$$\underbrace{\frac{dL(t)}{dt}}_{\text{LnCaP}} = \underbrace{-\delta L(t)}_{\text{cell death}} - \underbrace{k_t \alpha\big(A(t)\big)L(t)}_{\text{Differentiation to NE}} - \underbrace{\beta\big(L(t),A(t)\big)L(t)}_{\text{resting cells become proliferating}} + \underbrace{2\Big(1-k_p\alpha\big(A(t-\tau_1)\big)\Big)e^{-\delta\tau_1}\beta(L(t-\tau_1),A(t-\tau_1))L(t-\tau_1)}_{\text{newly born cells generated by asymmetric cell division}} \qquad (A.2)$$

$$\underbrace{\frac{dN(t)}{dt}}_{NE\text{-like cells}} = -\underbrace{\mu N(t)}_{\text{cell death}} + \underbrace{2k_p\alpha\big(A(t-\tau_1)\big)e^{-\delta\tau_1}\beta(L(t-\tau_1),A(t-\tau_1))L(t-\tau_1)}_{\text{NE generated by asymmetric cell division}} + \underbrace{k_t e^{-\delta\tau_2}\alpha\big(A(t-\tau_2)\big)L(t-\tau_2)}_{\text{Differentiation from L}} \qquad (A.3)$$

LNCaP cells have a constant *per capita* mortality rate $\delta$ and can differentiate into NE-like cells with an androgen-dependent rate $k_t\ \alpha(A)$, where $k_t$ represents the differentiation efficiency. Experiments proved that LNCaP trans-differentiation only occurs for low androgen levels. To capture this evidence, we represented the dependence of differentiation on the androgen with the Ricker function:

$$\alpha\big(A\big) = rA\,\mathrm{e}^{-aA}, \qquad (B)$$

which is a standard choice for bell-shaped patterns skewed to the right. The positive constants $r$ and $a$ respectively define the slope with which the differentiation rate increases, and the inverse of the differentiation rate maximum point ($1/a$). Experimental evidences suggested that the differentiation induced by androgen deprivation is delayed, we therefore assumed that differentiating cells need a time $\tau_2$ to perform all processes necessary to fully trans-differentiate in NE-like cells. The equation for trans-differentiating cells can be written as

$$\underbrace{\frac{dT(t)}{dt}}_{\text{differentiating cells}} = -\underbrace{\delta T(t)}_{\text{cell death}} + \underbrace{k_t\alpha(A(t))L(t)}_{\text{resting cells becoming differentiated}} - \underbrace{e^{-\delta\tau_2}k_t\alpha(A(t-\tau_2))L(t-\tau_2)}_{\text{cells fully differentiated}}, \qquad (A.4)$$

where $T(t)$ is the population size at time $t$. From equation (A.4) we can write

$$T(t)=\int_{t-\tau_2}^{t} e^{-\delta(t-s)}\alpha\big(A(s)\big)L(s)ds.$$

We also assumed that LNCaP cells population is divided into proliferating and quiescent/mature cells. LNCaP cells need a time $\tau_1$ to perform all processes required for cell division by mitosis, e.g., $\tau_1$ is the duration of cell cycle. The proliferating cells mortality rate is γ and, by the end of the mitotic phase, each cell has divided in two cells, which either are LNCaP entering in the quiescent phase or differentiated NE-like cells as previously reported (1). The equation for proliferating cells can be written as

$$\underbrace{\frac{dP(t)}{dt}}_{\text{poliferating cells}} = -\underbrace{\gamma P(t)}_{\text{cell death}} + \underbrace{\beta(L(t),A(t))L(t)}_{\text{resting cells becoming proliferating}} - \underbrace{e^{-\gamma\tau_1}\beta(L(t-\tau_1),A(t-\tau_1))L(t-\tau_1)}_{\substack{\text{proliferating cells}\\ \text{entering the resting phase}}}, \qquad \text{(A.5)}$$

where *P(t)* is the population size at time *t*. From equation (A.5) it follows that the proliferating cell population can be explicitly calculated as

$$P(t)=\int_{t-\tau_1}^{t} e^{-\gamma(t-s)}\beta\big(L(s),A(s)\big)L(s)ds.$$

The asymmetric cell division occurs at low androgen levels as described by Eq. (B), with $k_p$ representing its efficiency. The rate at which resting cells enter the proliferating phase depends both on level of androgen in the medium and cell density. We assumed that a high level of androgen aids proliferation of LNCaP cells (5), while a high cell density inhibits it. The model describing the resting-to-proliferative phase rate $\big(\beta(L,A)\big)$ consists of a continuous function that is zero in absence of androgen in the medium $\big(\beta(L,0)=0\big)$, increases as the androgen concentration increases, and decreases as the LNCaP cell concentration increases (1,2):

$$\beta(L,A) = \beta_0 \underbrace{\frac{\theta^n}{\theta^n + L^n}}_{\substack{\text{inhibition} \\ \text{by cell density}}} \underbrace{\frac{A}{b + A}}_{\substack{\text{androgen} \\ \text{dependence}}} . \qquad \text{(C)}$$

On the right hand side of Eq. (C), the first term represents the inhibition of the mitotic reentry rate ($\beta$, from $L(t)$ into $P(t)$) due to cell concentration and is described by a Hill function. The two positive constants $\theta$ and $n$ have similar roles to the Hill coefficients, and together they define the response to cell concentration changes. The second term is a Michaelis-Menten function where $b$ describes the androgen level at which $\beta$ is half. Finally, the positive constant $\beta_0$ represents the maximum rate of cell movement from the resting phase into proliferation, which is achieved in absence of the inhibition caused by low androgen levels or high cell concentrations.

The differentiated cells are post-mitotic and die with a mortality rate $\mu$. Androgen is assumed homogeneously distributed in the whole medium, and we do not differentiate between the intracellular and extracellular one. The exponent $\varphi$ controls the decay of androgen concentration in the medium, and NE-like cells secrete A-like factors with a constant rate $\kappa$.

Other authors such as Morken and colleagues (3) and Portz and colleagues (4) assumed that proliferation of prostate cancer cells is androgen dependent, but none of the existing models considered cell differentiation and its dependence on the androgen content, nor the possibility that differentiated cells could play an *active* role in sustaining the tumor in androgen deprived conditions. We could therefore consider these as the major novelties of this model.

## INTRODUCTION

Neuroendocrine (NE) cells are highly specialized neuron-like cells with peculiar secretory functions, which are widely scattered throughout the human body including non-neuroendocrine glands like prostate. In normal prostatic parenchyma, NE cells are part of a diffuse system that contributes to the homeostasis of the surrounding epithelial population (6). The NE system acts through its secreted products such as calcitonin, parathyroid hormone-related protein (PTHrP), chromogranins (CgA, CgB), neuron-specific enolase (NSE), neurotensin (NT), serotonin, bombesin and somatostatin (7). These peptide hormones and biogenic amines can either be released into the bloodstream or act locally by paracrine or autocrine signaling in an androgen-independent way (7). NE cells and the associated neuropeptides play also a crucial role in sustaining both growth and progression of many, if not all, conventional prostate adenocarcinomas (8,9) with a wide preclinical and clinical evidence of a poor prognosis correlation (10). However, the nature and the origin of NE cells in prostate tumor lesions and their underlying molecular mechanisms are still controversial. Most likely, this is due to the complex heterogeneity and the multifaceted way in which NE cells are linked to tumor progression. The ability of NE cell to induce an early onset of a hormone refractory status is very intriguing and clinically relevant. The transition from hormone-sensitive to hormone-insensitive status is one of the most critical issues in prostate cancer research as the conventional primary androgen-deprivation therapy is only transiently successful. Over a period of 16 to 18 months, the tumor progresses to a hormone independent status also known as castrate-resistant prostate cancer (CRPC). One emerging aspect of CRPC is that the AR signaling remains persistent. Based on the overall survival advantages, Food and Drug Administration recently approved the "secondary" hormone therapy when patients develop CRPC (11). The mechanisms that

upregulate intracellular androgens and/or androgen receptor (AR), leading to ongoing AR-directed cancer growth despite a castrate level of serum androgens are not understood yet. It is widely believed that trans-differentiation from an epithelial-like phenotype to an NE-like phenotype is due to the fall of androgen levels and to the block of steroid hormone action (6). This treatment-related NE-PCa is a resistance mechanism promoted by the hormonal therapy itself. The molecular processes, associated with the treatment related NE-PCa pathogenesis, are different from those observed in pure small-cell/neuroendocrine prostate cancer proving the existence of different types of NE cells (12,13). The incidence of NE trans-differentiation can be related to the duration of treatments. No relevant clonal propagation of NE cells has been reported after a short-term neoadjuvant androgen deprivation therapy (14), while significant increase of NE status was found in some of the patients who went through a long-term hormone-based treatment (15,16).

The application of "omics" sciences and mathematics to biological systems is the approach we propose to investigate how NE trans-differentiation contributes to tumor progression and hormone therapy failure in prostate cancer. We cultured androgen-dependent LNCaP cells in long-term hormone deprived conditions to allow the permanent trans-differentiation into a NE phenotype. We applied hierarchical clustering and multivariate statistical algorithms, including orthogonal projection to latent structure (O2PLS), to explore the effect of long-term hormone deprivation on transcripts and metabolites. We applied multivariate statistical analysis to find the correlations existing between metabolites and mRNA transcript levels in relation with cell phenotype. Finally, with a mathematical predictive model we investigated the intrinsic relationship between the two phenotypes under prolonged low hormone conditions.

## MATERIALS AND METHODS:

**Cell Culture and Neuroendocrine Trans-differentiation:** The human prostate carcinoma cell line LNCaP (clone FGC; CRL-1740™; passage number 10-40) was obtained from American Type Culture Collection (ATCC, Milan, Italy) in 2013. Morphology check by microscope and cell growth curves were performed routinely. Cells were cultured in RPMI medium supplemented with 10% heat-inactivated fetal bovine serum (FBS, Gibco-Invitrogen, Milan) according to the manufacturer's instructions in 37°C in a 5% $CO_2$-enriched humidified air atmosphere. In experiments assessing LNCaP neuroendocrine trans-differentiation protocol, cells were seeded at $4x10^5$ cells per 100mm dishes and left for 24 hours in regular media containing 10% heat-inactivated FBS (before switching to various differentiation media (RPMI medium supplemented with different percentages of dextran-coated-charcoal stripped FBS, dcc-str FBS, Sigma, Milan). Cells were maintained in those conditions until they started elongating their shape and activating a neuron-like morphology characterized by a progressive and sustained expression of neuroendocrine markers up to fourteen days. For the parameterization of the mathematical model, we differentiated LNCaP in 1% dcc-str-FBS (n=4) and counted cells (day 3-6-10 and 14) either with Burker chamber or with Millipore's Scepter automated handheld cell counter.

**NMR and PCR Data Integration:** $^1$H-NMR and PCR data were pre-treated with centering and unit variance scaling, respectively. Then we scaled the corresponding matrices to an equal total sum of squares to avoid the dominance of any of them. We integrated datasets by Orthogonal Projections to Latent Structures (O2PLS) in order to implement a bilinear statistical model and reveal joined variation. The influence of the original variables on the OPLS model were interpreted by inspection of the predictive regression coefficients, which are related to how each

variable influences the model for prediction of the response variables. We derived O2PLS models from both polar and lipophilic NMR data in correlation with PCR data. In order to identify the subset of most responsible metabolites and transcripts characterizing the trans differentiation process, variables were selected using a combination of VIP (Variable Influence in Projection) value >1 and correlation loadings pq[corr] >0.8 for the polar model. We also generated a correlation map with hierarchical clustering by combining transcript values and selected polar metabolite buckets where we considered Euclidean distance for the metrics and WARD method for clustering criterion.

**Pathway Analysis:** Pathway topology and biomarker analysis on selected and more representative metabolites in class separation were applied to the pathway topology search tool in Metaboanalyst 2.0 (17,18). We calculated the centrality through the Pathway Impact, a combination of the centrality and pathway enrichment results. Metabolites were selected by evaluating both VIP values > 1 in class discrimination and correlation values |pq[corr]| > 0.8. Homo sapiens pathway library was chosen and analyzed using Fisher's Exact Test for over representation and Relative-betweenness Centrality for pathway topology analysis.

**Formulation of the Mathematical Model:** The mathematical model introduced in the quick guide was used to describe laboratory experiments on the interaction between the human prostatic cancer cells LNCaP and the trans-differentiated NE-like cell population. Most of the mathematical models for PCa analyze the effects of continuous (19) or intermittent (20-25) androgen deprivation treatments on cancer progression. Prostatic tumor cells are usually divided in androgen dependent (AD) and androgen independent (AI), with AD transforming in AI in a reversible or irreversible way (25). In some models the mutation rate is considered directly dependent on the androgen concentration (4,19,21,25), while in others, the switch rate depends

on a cell quota of bound androgen receptor (3,4). All these studies investigate the well-known mechanism of androgen-independent relapse and do not consider cell trans-differentiation as such. Also, differently from the mathematical approach followed in other types of tumors, e.g. colonic crypt and colorectal cancer (26-28), in the case of prostate cancer the well-established theory of cancer stem cells, which assumes an asymmetrical cell division (29), has not been considered in the representation of tumor growth (1,30). In our model (A1 – A3) according with the cancer stem cell theory, we assumed that LNCaP mitosis leads to the formation of both undifferentiated and differentiated cells. The differentiation, which is driven by environmental factors (i.e. prolonged hormone depletion), is considered irreversible and differentiated cells apoptotic, as our experiments did not show any reversibility or proliferation of NE-like cells. The model also represents androgen dynamics. The experiments were run considering different percentages of charcoal stripped serum, however given the direct proportionality between the serum and its androgen content in the model we directly refer to androgen levels. Processes such as proliferation and trans-differentiation depend on the androgen level.

**Parameterization of the Mathematical Model:** The model was parameterized from data based on the experiments described above, and with values and ranges taken from the suitable literature when experimental data were not able to provide the required information. We took from the literature values for LNCaP and NE-like cell death rates $\delta$ and $\mu$, for the androgen degradation rate $\varphi$ (3), and for the Hill parameter $n$ (5). To parameterize the Ricker function, representing the relationship between androgen levels and trans-differentiation (Eq. (B)), we designed an experiment that would provide the maximum differentiation rate at different androgen levels. The non-linear regression of these data provided the following parameter values $r = 3 \pm 2$ day$^{-1}$

and $a = 1.3 \pm 0.3$ (Figure S1). The proliferation parameters $\beta_0 = 1.8 \pm 0.2$ day$^{-1}$ and $\theta = 0.9 \pm 0.1$ cells were estimated from empirical data of LNCaP grown in regular growth medium.

According to the manufacturer, the value for LNCaP cell cycle duration $\tau_1$ was set equal to 1.43 day, while the value of the delay in the differentiation process $\tau_2 = 7$ day was estimated from the progressive expression of NT over time (Figure 1). The value of the Michaelis-Menten half-saturation constant $b = 0.2$ was based on the observation that even at very low levels of androgen LNCaP cells are still able to proliferate (Figure 2). Finally the fit of 14-day experiments of LNCaP growth in androgen deprived conditions provided values for the differentiation efficiency $k_t = 0.6 \pm 0.2$, and the asymmetrical division parameter $k_p = 0.5 \pm 0.2$. Values for the parameter $\kappa$ were considered in the range of 0.003 to 0.03 day$^{-1}$. Numerical simulations and parameterization were performed with MATLAB R2014a.

**RESULTS:**

**Acquisition of Neuroendocrine Phenotype with Anti-proliferative Action on Parental LNCaP Cells:** To investigate the role of NE cells during AI acquisition we cultured androgen-dependent LNCaP cells in long-term hormone deprived conditions. Different culture conditions (from 0% to 5% dcc-srt FBS) were tested. Morphological and transcriptional data analyzed all over the 14-day experimental period, indicated the best differentiation medium for the study. Low androgen content rather than complete androgen depletion appeared to be crucial since the 1% rate was an exclusive condition for the occurrence of this cellular phenomenon. Only when hormone content was kept at 1% dcc-str FBS, cells started elongating their shape and showing a neuronal-like morphology. From day 1 to day 3 cells retained the typical LNCaP morphology, a spindle shape with occasional pseudopodium-like extensions. Starting from day 8-10, cells

presented an elongation of their shape that resolved (day 14) in the development of long-branched neuritic-like processes with small cell bodies (Figure 1A-1H). The elongating shapes were characterized by a progressive and sustained expression of neuroendocrine markers up to 14 days (i.e., NSE, NT) (Figure 1I and 1L). In order to investigate paracrine interactions between the two cellular phenotypes, we determined the effect of NE conditioned media on LNCaP cell growth by means of [$^3$H]-Thymidine incorporation. LNCaP cells were exposed (48 hours) to various conditioned media collected during NE trans-differentiation at different time points (see Scheme in Figure 2). DNA synthesis of LNCaP cells was significantly ($p < 0.001$) affected by the complete deprivation of serum (non-serum medium, NSM), while non-conditioned differentiation medium (DM) showed no per se effect when compared to regular growth medium (GM) (Figure 2A). Already after three days we observed that conditioned DM significantly ($p < 0.01$) inhibited [$^3$H]-Thymidine incorporation of LNCaP cells (Figure 2B).

**NMR and PCR based PCA Discriminates Classes Revealing a Non-malignant Phenotype:** NMR and PCR analyses were performed in parallel on LNCaP (day 0) and NE-like cells (day 14). Conspicuous differences were found in their metabolic profiles. In particular, some hydrophilic signals, commonly identified as prostate cancer biomarkers (31), such as creatine and phosphocreatine (Cr+PCr), glycine (Gly) and alanine (Ala), were mostly prominent in LNCaP compared to NE-like samples (Figure 3A). Also, the hydrophobic fraction denoted a different and phenotype-based distribution of total cholesterol content (Figure 3B). Free cholesterol was more pronounced in NE cells while, the form prevailing in LNCaP cells was the esterified one (Figure 3 C and D), recently related to prostate cancer aggressiveness (32). Differences were also found in the relative quantification of selected gene expression. The applied prolonged hormone deprived conditions led to a significant up-regulation of common

neuroendocrine secretory products (i.e., NSE, NT and CgA). While other hormone-related targets (i.e., estrogen receptor GPER and androgen-regulated channel TRPM8) were up regulated in NE-like cells, the expression of the prostatic tumor biomarker alpha-methyl-acyl-CoA racemase (AMACR) was strongly reduced in respect to LNCaP cells (Figure 4). Also, mRNA levels of a common indicator of PCa (i.e., PSA) were significantly mislaid in NE trans-differentiated cells when compared with parental malignant cells. The trans-differentiation process (Figure 4) did not affect gene expression of androgen receptor (AR). Both, NMR-based metabolic profiles and PCR-based analysis of relevant genes indicated that androgen deprivation drove the development to a less-malignant neuroendocrine phenotype. Accordingly, PCA applied both to NMR and PCR data smoothly discriminated androgen-dependent LNCaP cells from their relative trans-differentiated NE-like cells. The complete separation between classes was achieved with an unsupervised analysis (Figure S2).

**Data Integration and Joint Systematic Variation Suggests the Use of Healthy NE Biomarkers as Putative Indicators of Androgen-independent PCa:** Once we established a clear discrimination between the two phenotypes, we explored the shared variance between NMR and PCR values via O2PLS. In this way, we pointed out those variations that consistently and concurrently occurred during the trans-differentiation process (Figure 5A). The joint predictive structure showed that 95% of the variation in the polar NMR block (66% for lipid dataset) correlates with 96% of the variation in the transcript block (72% for lipid dataset), which is a substantial overlap. This approach produced a functional model for interchangeable predictions between NMR and PCR data. Class discrimination was achieved by considering the shared variation between transcripts and metabolites. We found a close linking between the two biological information sets (see regression coefficients in Figure S3) via O2PLS analysis that

displays sample scores and variable loadings in a joint predictive model (leave-one-out classification approach showed that only 3/10 samples were outliers). This model allows projecting the transcripts and metabolites on a common 2D plane (Figure 5A), where the positions describe the cell phenotype and the proximity between transcripts and metabolites relates with the correspondence of their changes. The analysis revealed that both PSA and AMACR, highly expressed in LNCaP cells, positively correlated with Cr+PCr, Gln, Pro and Ala. These transcripts also positively correlated with fatty acids (FAs) and phospholipidic compound (PC and PE) in LNCaP cells. We found minor positive correlations for choline and ethanolamine moieties (PE and GPC) and nucleoside derivatives (ribose and UDPG). Moreover, all the genes up regulated in NE-like population (i.e., TRPM8, CgA and GPER) correlated with Gln, *myo*-inositol (*myo*-Ins) and citrate (Cit). We observed different correlations for the two genes associated with the neuroendocrine phenotype. Individually NSE appeared correlated to PE/PC, Gln and GSH, while NT was mostly influenced by *myo*-Ins and acetate (Ace). Interestingly, NE-like cell population appeared mainly characterized by the joint variation of NT and GPER with free cholesterol. We used a correlation matrix based hierarchical clustering (CMBHC) for visualization purposes. The results of hierarchical clustering were then visualized as a tree structure plot (dendogram), which clearly classified the two cell populations based on transcripts and metabolites correlation coefficients (Figure 5B). As a final point, we applied Metabolite Set Enrichment Analysis (MSEA) in order to draw biological inferences about selected metabolites and to identify their relevance in significant metabolic pathways. The applied selection showed that at least 30 major metabolic pathways were involved (Table S1). Among these, Alanine/Aspartate/Glutamate ($p = 1.81\ E^{-4}$, impact = 0.52); Glutamine/Glutamate ($p = 1.22\ E^{-03}$, impact = 0.35); Glutathione ($p = 1.45\ E^{-02}$, impact = 0.24); Glycine/Serine/Threonine (p = 1.44

$E^{-03}$, impact = 0.19); Arginine/Proline (p = 3.95 $E^{-4}$, impact = 0.13) metabolisms emerged. Considering both Holm p values and the False Discovery Rate (FDR) correction, we focused on Alanine/Aspartate/Glutamate metabolism (Holm p = 1.39 $E^{-02}$, FDR = 3.62 $E^{-03}$), which appeared to be the most affected between cell populations, with Glutamine/Glutamate metabolism (Holm p = 9.17 $E^{-02}$, FDR = 1.63 $E^{-02}$) to a minor extent (Figure 6).

**Mathematical Modeling of Neuroendocrine Trans-differentiation Supports a Self-sustaining Mechanism for LNCaP Cells:** Based on the experimental evidence we developed a mathematical model of LNCaP cells dynamics and trans-differentiation. We assumed a mechanism of androgen production by NE-like cells, and lack of androgen sources external to the system (see Eq. 1.1-1.3). Two types of analyses were applied, one to describe the cell growth dynamics (descriptive) and the other to forecast future behaviors (predictive). The descriptive analysis well represented all the outcomes of the *in vitro* experiments. The obtained growth curve, resembled the increase in cell numbers (from $3x10^5$ cells at day 0 to $2.5x10^6$ cells at day 16) measured as described above. (Figure 7A). Figure 7B shows the gradual acquisition of a neuroendocrine phenotype over time as we obtained from both morphological and transcriptomic analyses. The predictive analysis allowed a comparison between the outcome of the model and the results of a continuous androgen deprivation therapy. Keeping the same parameter values tuned on data from the 14-day experiment (Table S2), we ran a simulation for 400 days (Figure 7C and 7D). After a first period of approximately 150 days, during which LNCaP cells almost appeared extinguished while NE-like cells were nearly constant in number, the system behavior suddenly changed and NE-like cell population density started increasing followed by an increase of LNCaP cells (Figure 7D). Both populations reached a steady state after further 150 days. The simulations showed how LNCaP cells self-sustain by enhancing a concentration of NE-like cells

sufficient to produce enough A-like factor to allow androgen-dependent cell proliferation (Figure 7C).

**DISCUSSION:**

Despite the advances in early detection due to a widespread use of PSA-based screening, a high rate of patients still presents locally advanced PCa when diagnosed. Furthermore, most of the patients who successfully go through endocrine therapy are often at high risk of recurrence. This unfavorable prognosis is due to the progression of primarily androgen-independent cancer cells that escape hormonal ablation. NE trans-differentiation is one of the hallmarks of this phenomenon; nonetheless, the clinical significance of the coexistence of NE phenotype in the context of classic PCa is still controversial. The approach we proposed in this study is based on the use of "omics" sciences and mathematics to investigate how NE trans-differentiation contributes to tumor progression and hormone therapy failure. A growing body of literature describes NE trans-differentiation from LNCaP cells as a result of short-term (72 hours) androgen withdrawal, or a dramatic increase of c-AMP levels, or a cytokine-based induction. Those cells were described as cancerous terminally transdifferentiated NE cells lacking of AR and PSA expression. Herein, differently from previously described *in vitro* protocols (33,34), we cultured androgen-dependent LNCaP cells in a long-term (up to 14 days) hormone deprived conditions. Such conditions led to a possibly closer "human-like" model of androgen resistance. Unexpectedly, metabolic profiles revealed that LNCaP cells trans-differentiated into a non-malignant neuroendocrine phenotype, resembling a clinically positive response to primary androgen deprivation therapy. Experiments also showed that some environmental factors (i.e., minimal androgen content rather than its depletion) are crucial for this particular trans-

differentiation process. NE conditioned media (collected at various days of the trans-differentiation process) affected LNCaP cell proliferation. However, further investigations are needed to clarify if the reduction of LNCaP cells is only due the androgen-depleted conditions or if there is a concurrent NE-mediated anti-mitogenic effect.

Metabolome analysis described the dynamic changes in the pattern of malignancy observed during the considered experimental period. LNCaP cells ($day_0$) were characterized by Ala, Glu, Cr and Gly (the precursor of sarcosine) previously described as PCa metabolic biomarkers (35-37). In agreement with the well-known Warburg effect (38), these cells showed an increased rate of energetic expenditure, as the relevance of metabolic-related nucleosides (i.e., AMP, NADP, NAD, ATP, UDP) indicates. PCa generally presents a high glucose oxidation and low levels of *myo*-inositol (39,40), so the increase in glutathione (in its reduced form, GSH), Gln and *myo*-inositol signals observed in NE-like cells at day 14 is a further confirmation of their non-malignant phenotype. NE cells exhibited high levels of cholesterol, the precursor of the entire androgen synthesis cascade. Very recently has been reported that an aberrant accumulation of its esterified form is related to prostate cancer aggressiveness (32). However, the abundance of cholesterol in $day_{14}$ cells was mostly due to its free and not esterified form, which instead resulted more pronounced in LNCaP $day_0$ cells. Moreover, enriched pathway analysis showed that the Alanine/Aspartate/Glutamate metabolism was the most profoundly affected during trans-differentiation. In particular, we found that androgen deprivation produced a down regulation of L-Asp in NE-like cells. This finding are in agreement with the reported evidence that in prostate epithelial cells, L-Asp is an important source for citrate synthesis via oxaloacetate through testosterone positively regulated L-Asp transporter (41). The two cell populations under study showed distinct transcripts related to their phenotypes (up-regulation of PSA and AMACR in

$day_0$-cells, and up-regulation of NSE, NT and CgA in $day_{14}$-cells, respectively). Furthermore, under low serum condition non-malignant NE-like cells exhibited a higher content of hormone-related targets (GPER and TRPM8) that could be related with the induction of androgen independence in adjacent malignant phenotype. TRPM8, in fact, is positively regulated by androgens, and we showed how NE cells under persistent low levels of hormones can increase the production of free-cholesterol, precursor of testosterone. We did not observe a parallel reduction of AR expression in trans-differentiated NE $day_{14}$ cells. This can be explained assuming that the abundance of free cholesterol found in NE cells sustains the expression of AR even in low androgen conditions.

We applied a descriptive *in silico* analysis to represent the trans-differentiation process and to further investigate the possible role of non-malignant camouflaged NE cells on potential PCa relapse. The mathematical model we developed combined all information provided by experiments and statistical analysis, and the numerical simulations well represented the outcomes of the 14-day experiments. Predictive analyses provided a possible explanation to the reason why tumorigenic LNCaP cells differentiate into non-malignant NE-like cells. In fact, long-term simulations showed a peculiar ability of NE cells in sustaining the system. Numerical results also provided a possible reason why most patients but not all develop androgen resistant prostate cancer, as the simulated outcome depended on the initial size of LNCaP cell population and on an eventual minimum size for the NE-like cell population. The key assumption for the model behavior is that NE-like cells have a putative role in hormonally treated cancers by releasing paracrine factors that promote residual prostate cancer cell growth and progression (NE-based feeding-support).

Given the *in silico* results we can assert that malignant androgen-dependent LNCaP cells react to hormone deprivation by favoring the establishment of a non-malignant NE cell population. We can consider these NE cells as "hidden" androgen-resistant clones coexisting with scattered malignant cells. This apparent positive response to early hormone-based therapy leads to the increase of NE components, which, over time, show their "evil-side" by thrusting the recovery of malignant LNCaP proliferation through a paracrine mechanism.

In conclusion, we produced an original *in vitro* model to investigate the pathophysiology of NE cells in hormone-refractory transition of PCa. The non-malignant phenotype achieved in our model represents an intriguing link between NE cell differentiation and the occurrence of hormone refractory PCa status. These AI cells are able to recover the proliferation index of surrounding non-NE phenotype cancer cells by the secretion of NE products through a paracrine mechanism. The predictive forecasts of the mathematical model support the notion that, also in a clinical setting, treatment related NE cells generate tardive inductive stimuli on quiescent/undetectable tumor cells. The statistical analyses provided a link between transcripts and metabolites that were highly co-responsible for class distinction. All the found correlations are important for the future development of new diagnostic tools for androgen-independent PCa. Translated into a clinical setting this bidirectional model could be used for predictions in both directions between NMR and PCR data matrices, offering new possibilities of monitoring the response of PCa patients to treatments. Further *in vivo* analyses are required a) to validate new putative biomarker candidates during the follow up of treated PCa and b) to elucidate the feasibility of this complex functional network between epithelial PSA secretory cells and "dual face" neuroendocrine cells. The understanding of the biological duality of these NE cells, with a non-malignant phenotype that "sneakily" sustains hormone-dependent tumor cells, will be

clinically relevant in the management of advanced, relapsing and castration-resistant PCa as well as in the development of new strategies for targeted therapies and/or diagnostic biomarkers.

**ACKNOWELDGMENTS:** The authors thank Luigia Cristino and Roberta Imperatore for their expert technical assistance in microscopic image acquisition, and Pierangelo Orlando for the help provided in some of the molecular biology analyses herein presented.

**Author contributions:** A.L. designed research; D.P., M.C., D.M., F.A.I., E.M., R.V., A.M. performed research; A.L., D.P. and M.C. analyzed data and wrote the paper.

**REFERENCES:**

1. Adimy M, Crauste F, Marquet C. Asymptotic behavior and stability switch for a mature–immature model of cell differentiation. Nonlinear Analysis: Real World Applications 2010;11(4):2913-29.

2. Adimy M, Crauste F, Ruan S. Modelling hematopoiesis mediated by growth factors with applications to periodic hematological diseases. BULLETIN OF MATHEMATICAL BIOLOGY 2006;68(8):2321-51.

3. Morken JD, Packer A, Everett RA, Nagy JD, Kuang Y. Mechanisms of resistance to intermittent androgen deprivation in patients with prostate cancer identified by a novel computational method. Cancer Res 2014;74(14):3673-83.

4. Portz T, Kuang Y, Nagy J. A clinical data validated mathematical model of prostate cancer growth under intermittent androgen suppression therapy. AIP Advances 2012;2(011002):1-14.

5. Eikenberry SE, Nagy JD, Kuang Y. The evolutionary impact of androgen levels on prostate cancer in a multi-scale mathematical model. Biol Direct 2010;5:24.

6. Terry S, Beltran H. The many faces of neuroendocrine differentiation in prostate cancer progression. Front Oncol 2014;4(60):1-9.

7. Perrot V. Neuroendocrine Differentiation in the Progression of Prostate Cancer: An Update on Recent Developments. Open Journal of Urology 2012;2:173-82.

8. Bonkhoff H. Neuroendocrine differentiation in human prostate cancer. Morphogenesis, proliferation and androgen receptor status. Ann Oncol 2001;12 Suppl 2:S141-4.

9. Hansson J, Abrahamsson PA. Neuroendocrine pathogenesis in adenocarcinoma of the prostate. Ann Oncol 2001;12 Suppl 2:S145-52.

10. Berruti A, Vignani F, Russo L, Bertaglia V, Tullio M, Tucci M, et al. Prognostic role of neuroendocrine differentiation in prostate cancer, putting together the pieces of the puzzle. Open Access J Urol 2010;2:109-24.

11. Taplin ME. Secondary Hormone Therapy for Castration-Resistant Prostate Cancer. Oncology (Williston Park) 2013;27(5).

12. Beltran H, Tagawa ST, Park K, MacDonald T, Milowsky MI, Mosquera JM, et al. Challenges in recognizing treatment-related neuroendocrine prostate cancer. J Clin Oncol 2012;30(36):e386-9.

13. Knudsen KE, Scher HI. Starving the addiction: new opportunities for durable suppression of AR signaling in prostate cancer. Clin Cancer Res 2009;15(15):4792-8.

14. Kollermann J, Helpap B. Neuroendocrine differentiation and short-term neoadjuvant hormonal treatment of prostatic carcinoma with special regard to tumor regression. Eur Urol 2001;40(3):313-7.

15. Jiborn T, Bjartell A, Abrahamsson P. Neuroendocrine differentiation in prostatic carcinoma during hormonal treatment. Urology 1998;51(4):585-89.

16. Hirano D, Okada Y, Minei S, Takimoto Y, Nemoto N. Neuroendocrine differentiation in hormone refractory prostate cancer following androgen deprivation therapy. Eur Urol 2004;45(5):586-92; discussion 92.

17. Xia J, Mandal R, Sinelnikov IV, Broadhurst D, Wishart DS. MetaboAnalyst 2.0--a comprehensive server for metabolomic data analysis. Nucleic Acids Res 2012;40(Web Server issue):W127-33.

18. Xia J, Psychogios N, Young N, Wishart DS. MetaboAnalyst: a web server for metabolomic data analysis and interpretation. Nucleic Acids Res 2009;37(Web Server issue):W652-60.

19. Jackson T. A mathematical model of prostate tumor growth and androgen-independent relapse. DISCRETE AND CONTINUOUS DYNAMICAL SYSTEMS SERIES B 2004;4(1):187-202.

20. Tao Y, Guo Q, Aihara K. A partial differential equation model and its reduction to an ordinary differential equation model for prostate tumor growth under intermittent hormone therapy. J Math Biol 2013;(online published) 10.1007/s00285-013-0718-y.

21. Ideta A, Tanaka G, Takeuchi T, Aihara K. A mathematical model of intermittent androgen suppression for prostate cancer. Journal of nonlinear science 2008;18(6):593-613.

22. Hirata Y, Bruchovsky N, Aihara K. Development of a mathematical model that predicts the outcome of hormone therapy for prostate cancer. Journal of theoretical biology 2010;264(2):517-27.

23. Tao Y, Guo Q, Aihara K. A model at the macroscopic scale of prostate tumor growth under intermittent androgen suppression. Mathematical Models and Methods in Applied Sciences 2009;19(12):2177-201.

24. Guo Q, Tao Y, Aihara K. Mathematical modeling of prostate tumor growth under intermittent androgen suppression with partial differential equations. International Journal of Bifurcation and Chaos 2008;18(12):3789-96.

25. Tanaka G, Hirata Y, Goldenberg S, Bruchovsky N, Aihara K. Mathematical modelling of prostate cancer growth and its application to hormone therapy. Philosophical Transactions of the Royal Society A: Mathematical Physical and Engineering Sciences 2010;368(1930):5029-44.

26. Di Garbo A, Johnston M, Chapman S, Maini P. Variable renewal rate and growth properties of cell populations in colon crypts. Phys Rev E Stat Nonlin Soft Matter Phys 2010;104(10):4008-13.

27. d'Onofrio A, Tomlinson I. A nonlinear mathematical model of cell turnover differentiation and tumorigenesis in the intestinal crypt. Journal of theoretical biology 2007;244(3):367-74.

28. Johnston M, Edwards C, Bodmer W, Maini P, Chapman S. Mathematical modeling of cell population dynamics in the colonic crypt and in colorectal cancer. Proc Natl Acad Sci U S A 2007;104(10):4008-18.

29. Sottoriva A, Sloot P, Medema J, Vermeulen L. Exploring cancer stem cell niche directed tumor growth. Cell Cycle 2010;9(8):1472-79.

30. Quinn T, Sinkala Z. Dynamics of prostate cancer stem cells with diffusion and organism response. Biosystems 2009;96(1):69-79.

31. McDunn JE, Li Z, Adam KP, Neri BP, Wolfert RL, Milburn MV, et al. Metabolomic signatures of aggressive prostate cancer. Prostate 2013;73(14):1547-60.

32. Yue S, Li J, Lee SY, Lee HJ, Shao T, Song B, et al. Cholesteryl ester accumulation induced by PTEN loss and PI3K/AKT activation underlies human prostate cancer aggressiveness. Cell Metab 2014;19(3):393-406.

33. Wang Q, Horiatis D, Pinski J. Inhibitory effect of IL-6-induced neuroendocrine cells on prostate cancer cell proliferation. Prostate 2004;61(3):253-9.

34. Yuan TC, Veeramani S, Lin MF. Neuroendocrine-like prostate cancer cells: neuroendocrine transdifferentiation of prostate adenocarcinoma cells. Endocr Relat Cancer 2007;14(3):531-47.

35. Tessem M, Swanson M, Keshari K, Albers M, Joun D, Tabatabai Z, et al. Evaluation of lactate and alanine as metabolic biomarkers of prostate cancer using 1H HR-MAS spectroscopy of biopsy tissues. Magn Reson Med 2008;60(3):510-16.

36. Weinstein SJ, Mackrain K, Stolzenberg-Solomon RZ, Selhub J, Virtamo J, Albanes D. Serum creatinine and prostate cancer risk in a prospective study. Cancer Epidemiol Biomarkers Prev 2009;18(10):2643-9.

37. Khan AP, Rajendiran TM, Ateeq B, Asangani IA, Athanikar JN, Yocum AK, et al. The role of sarcosine metabolism in prostate cancer progression. Neoplasia 2013;15(5):491-501.

38. Munoz-Pinedo C, El Mjiyad N, Ricci JE. Cancer metabolism: current perspectives and future directions. Cell Death Dis 2012;3:e248.

39. Serkova NJ, Gamito EJ, Jones RH, O'Donnell C, Brown JL, Green S, et al. The metabolites citrate, myo-inositol, and spermine are potential age-independent markers of prostate cancer in human expressed prostatic secretions. Prostate 2008;68(6):620-8.

40. Traverso N, Ricciarelli R, Nitti M, Marengo B, Furfaro AL, Pronzato MA, et al. Role of glutathione in cancer progression and chemoresistance. Oxid Med Cell Longev 2013;2013:972913.

41. Lao L, Franklin RB, Costello LC. High-affinity L-aspartate transporter in prostate epithelial cells that is regulated by testosterone. Prostate 1993;22(1):53-63.

## FIGURE LEGENDS

**Figure 1:** Representative micrographs acquired by differential interference contrast showing cell morphology changes during trans-differentiation process. From day 1 (A and higher magnification in B) to day 3 (C and higher magnification in D), cells retain typical LNCaP morphology with spindle shape and occasional pseudopodium-like extensions. From day 8 (E and high magnification in F) to day 14 (G and high magnification in H), cells exhibit an elongation of their shape characterized by the development of long-branched neuritic-like processes with small cell bodies. Scale bar= 20 μm in A,C,E,G and 10 μm in B,D,F,H. The acquisition of neurite-like morphology was characterized by a progressive and sustained expression of neuroendocrine markers (neuron-specific enolase, NSE and neurotensin, NT) up to fourteen days.

**Figure 2:** Schematic representation of LNCaP neuroendocrine trans-differentiation. NE-conditioned media were pooled all along the differentiation protocol and later used to growth LNCaP cells in presence of [$^3$H]-Thymidine. (A) Effect of various media on LNCaP cell

proliferation. (B) Effect of NE-conditioned media on LNCaP cell proliferation. Data are reported as mean ± SD of two experiments in quadruplicate. GM = regular growth medium; DM = differentiation medium; NSM = non-serum medium. (*** indicates $p< 0.001$ *vs.* GM; ** indicates $p<0.01$ *vs.* DM; one-way ANOVA followed by Dunnett's Multiple Comparison Test, n=8).

**Figure 3:** NMR-based metabolome analysis. (A) Representative $^{1}$H-NMR spectra of LNCaP and NE cells polar extracts. (B) Representative $^{13}$C-NMR spectra of LNCaP and NE cells lipid extracts. (C-D) Bucket variations relative to (C) free cholesterol and (D) esterified cholesterol content in LNCaP and NE lipophilic fractions. Bin values are normalized to the total spectral area intensity. Abbreviations: MI, myo-inositol; Glu, glutamate; Gln, glutamine; Lac, lactate; Ala, alanine; Leu, leucine; Cr/PCr, creatine/phosphocreatine; Gly, glycine; Tau, taurine; Pro, proline; Ac, acetate; Val, valine; SFA, satured fatty acid; Chol, free cholesterol; Chol E, esterified cholesterol.

**Figure 4:** Transcript levels of androgen receptor (AR), G protein-coupled estrogen receptor 1 (GPER), alpha-methylacyl-CoA racemase (AMACR), transient receptor melastatin 8 (TRPM8), glycoprotein hormones alpha (CgA), neuron specific enolase (NSE), neurotensin (NT) and prostate-specific antigen (PSA) in parental LNCaP (day 0) and NE cells (day 14). All q-PCR analyses were performed in triplicate for at least three different biological preparations. Data are expressed using the $2^{-\Delta Ct}$ formula.

**Figure 5:** O2PLS and HMCB analysis for data integration. (A) O2PLS correlation plot displaying sample scores and variable loadings in a joint predictive model. Sample positions on the horizontal axis provide class separation. The proximity of variables (metabolites and transcripts) measures their mutual influence (covariation). Only the most influent variables, (VIP

>1 and pq[1]corr > 0.8) are labeled with their chemical shifts (metabolites) or names (transcripts). (B) Correlation map based on Pearson correlation coefficients between metabolites and transcripts. Rows and columns are rearranged according to the WARD-based correlation matrix based hierarchical clustering (CMBHC). Blue tones colored areas indicate positive correlations between NMR and PCR variables, while red tones indicate negative correlations between the same variables.

**Figure 6:** (A) Topology-based pathway analysis showing metabolic networks potentially affected during NE trans-differentiation. The most impacted metabolic pathways are specified by the volume and the color of the spheres (yellow least relevant, red most relevant) according to their statistical relevance p and impact value. (B) Metabolic scheme reporting Alanine, Aspartate and Glutamate pathway potentially affected during the NE trans-differentiation process.

**Figure 7:** Mathematical simulations of cell behavior over time. (A) Total cell number plotted against experimental counting. (B) Numerical simulation of LNCaP trans-differentiation into NE cells, as reported from the experimental outcome. (C) Predictive simulation of androgen-like factor over a time interval of 400 days. (D) Predictive simulation of LNCaP/NE cell system over a time interval of 400 days.

Figure 1

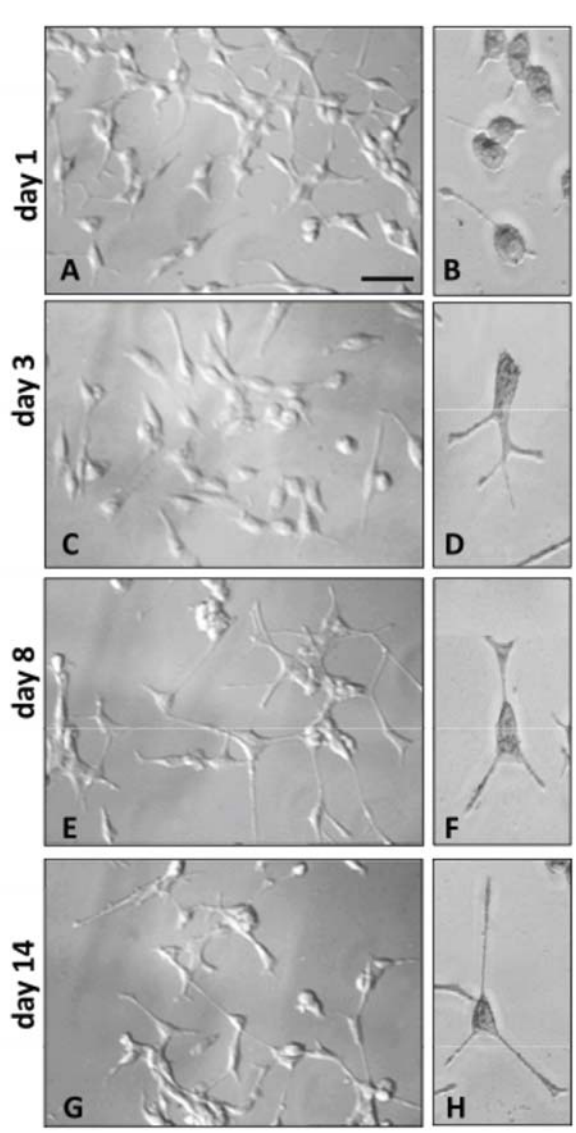


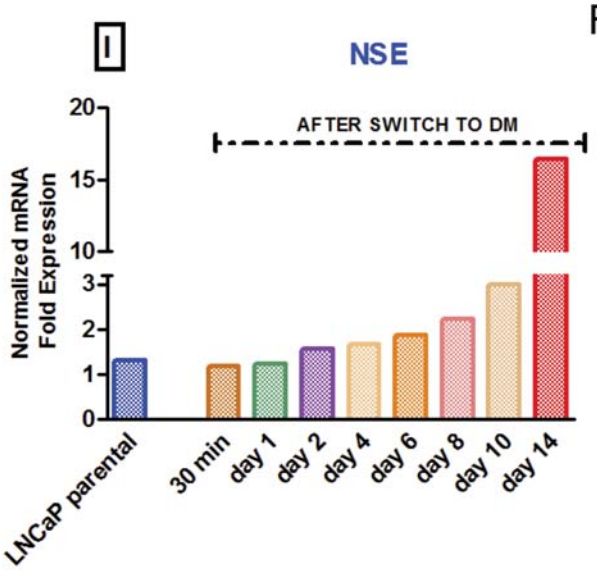


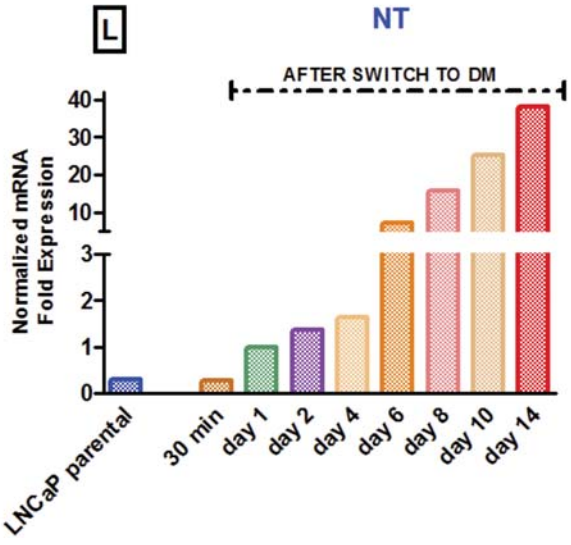

Figure 2

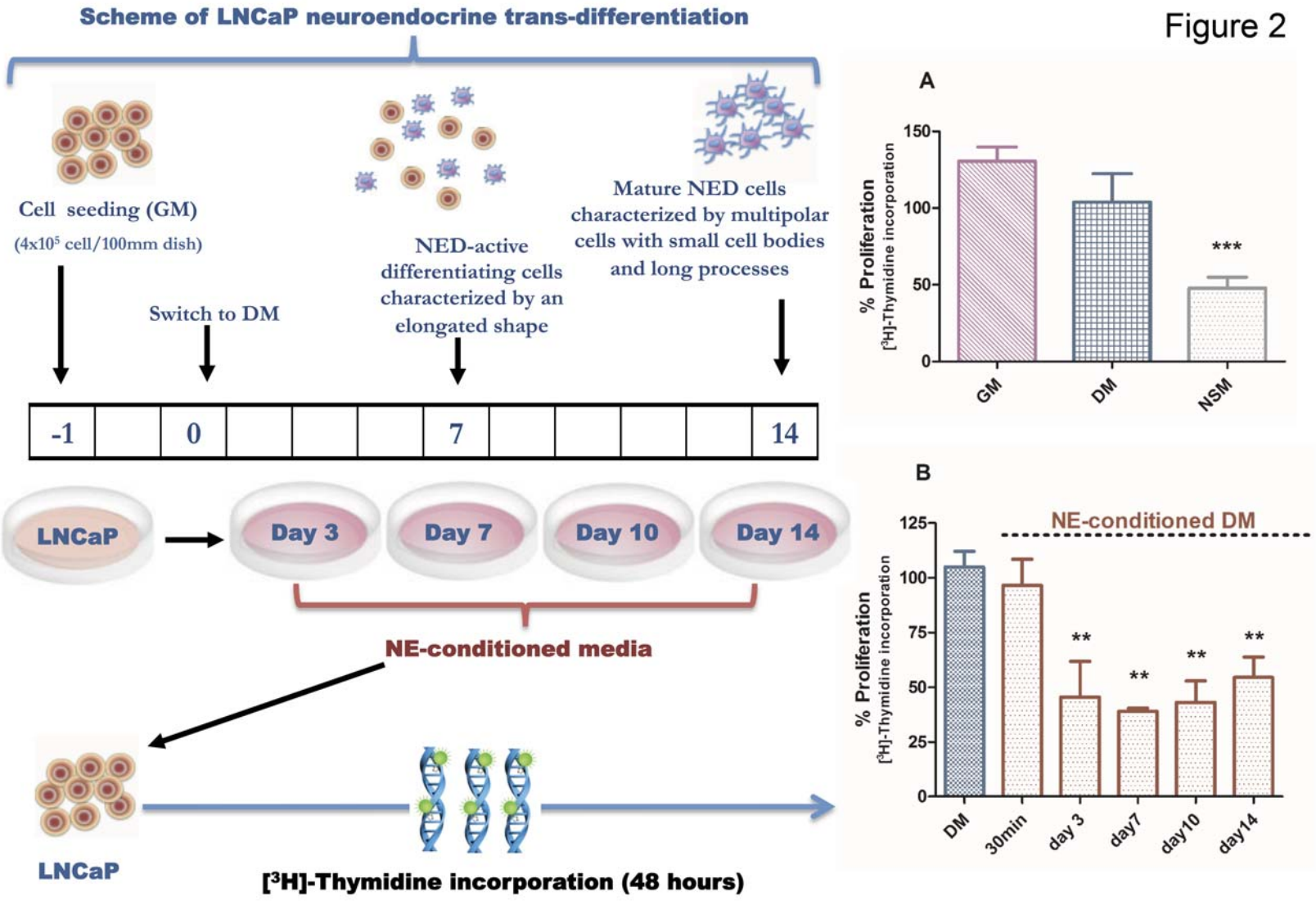

Author Manuscript Published OnlineFirst on June 11, 2015; DOI: 10.1158/0008-5472.CAN-14-3830
Author manuscripts have been peer reviewed and accepted for publication but have not yet been edited.

Figure 3

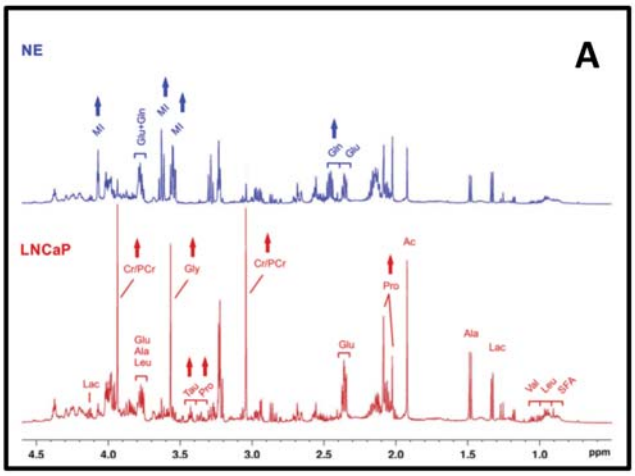


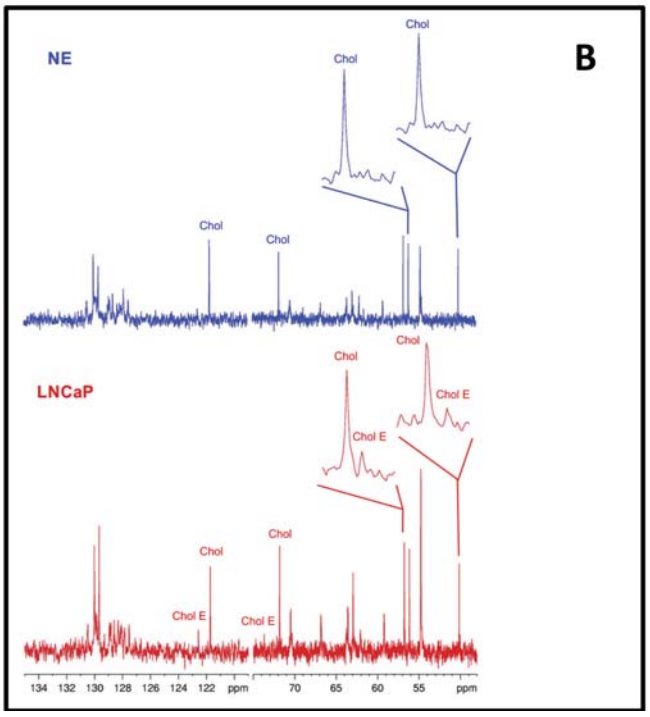


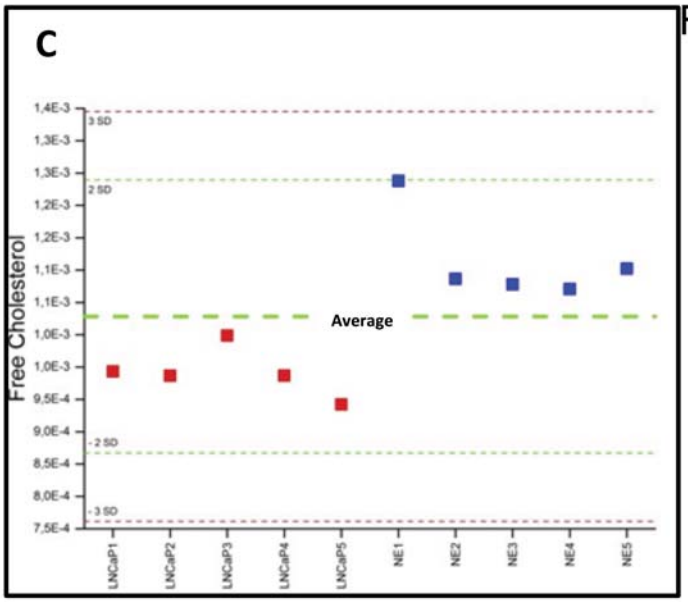


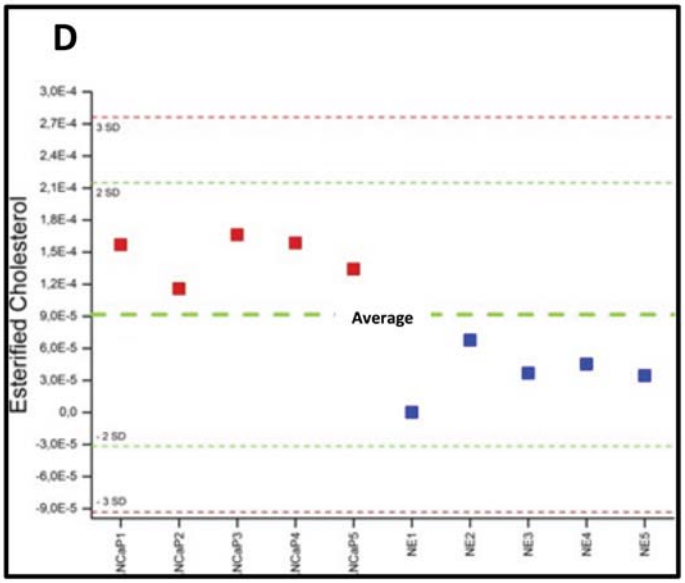

Author Manuscript Published OnlineFirst on June 11, 2015; DOI: 10.1158/0008-5472.CAN-14-3830


Figure 4

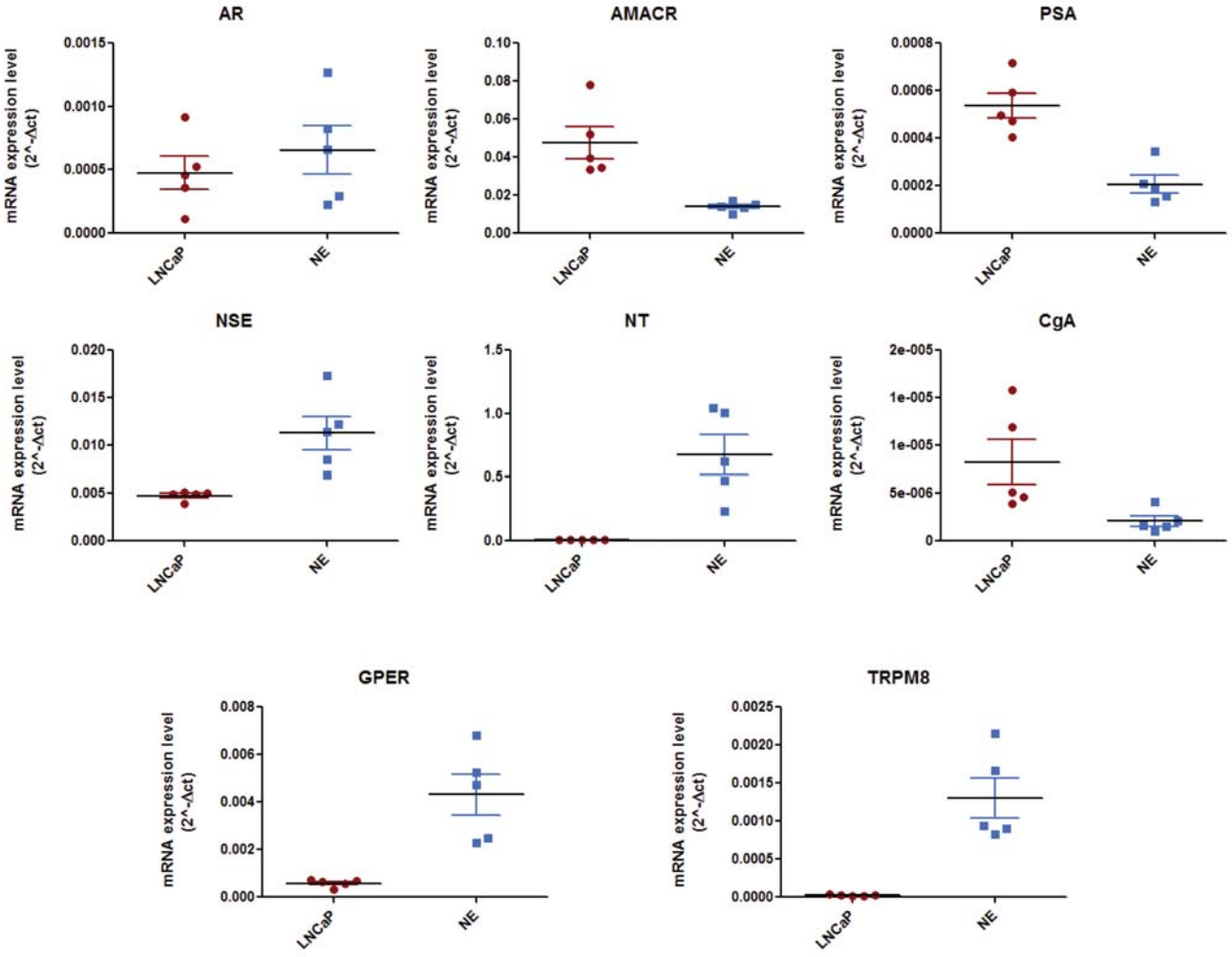

Author Manuscript Published OnlineFirst on June 11, 2015; DOI: 10.1158/0008-5472.CAN-14-3830
Author manuscripts have been peer reviewed and accepted for publication but have not yet been edited.

Figure 5

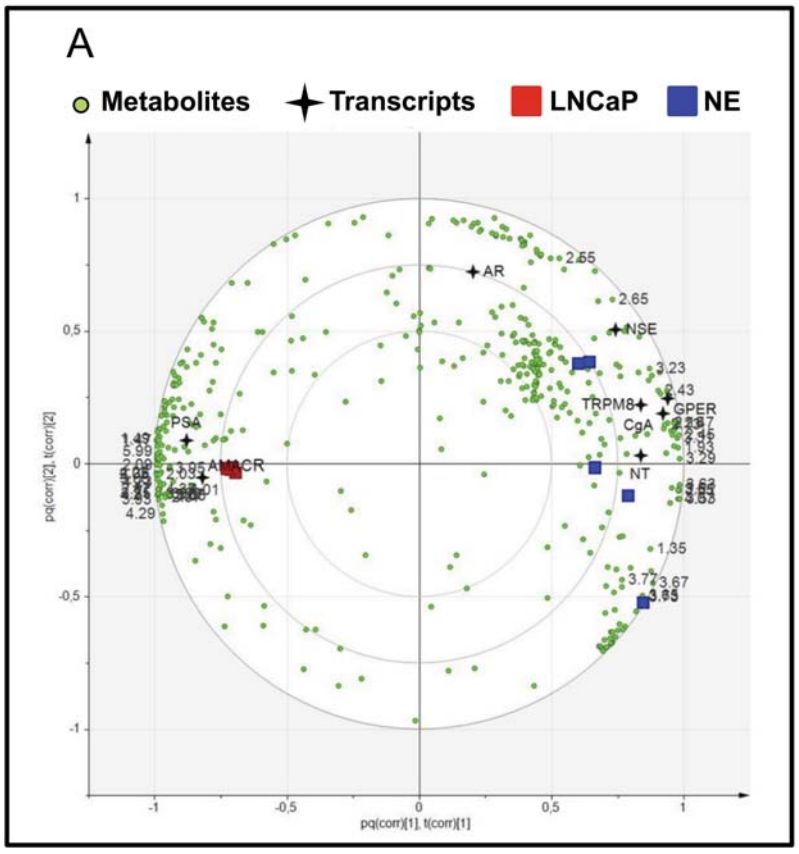


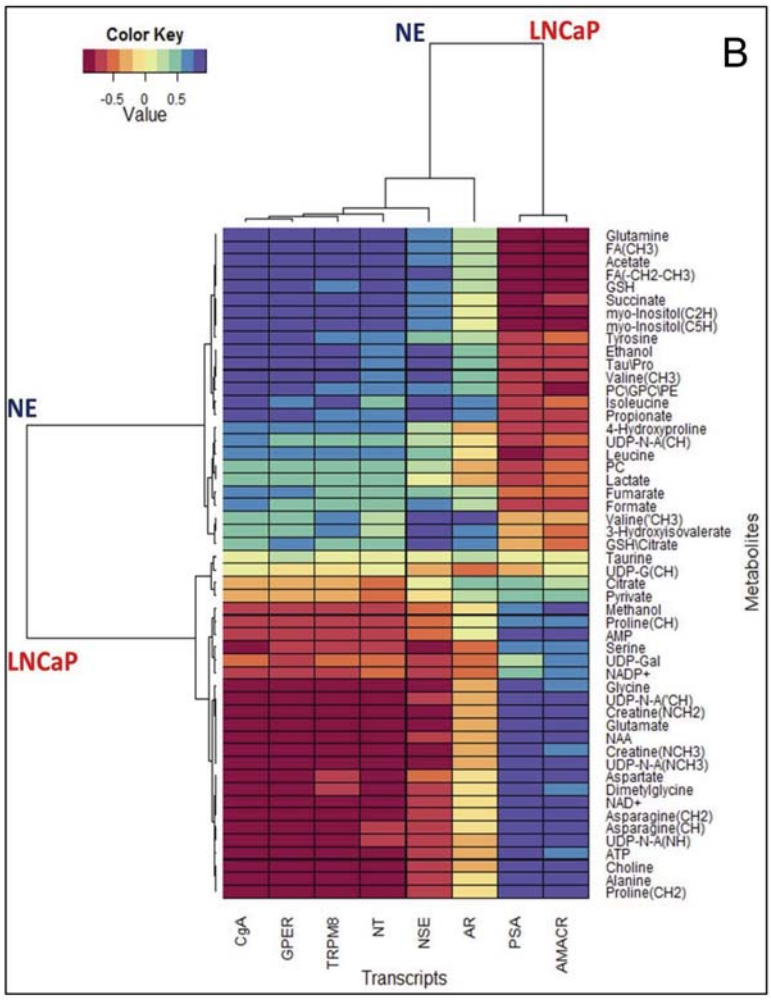

Author Manuscript Published OnlineFirst on June 11, 2015; DOI: 10.1158/0008-5472.CAN-14-3830
Author manuscripts have been peer reviewed and accepted for publication but have not yet been edited.

Figure 6

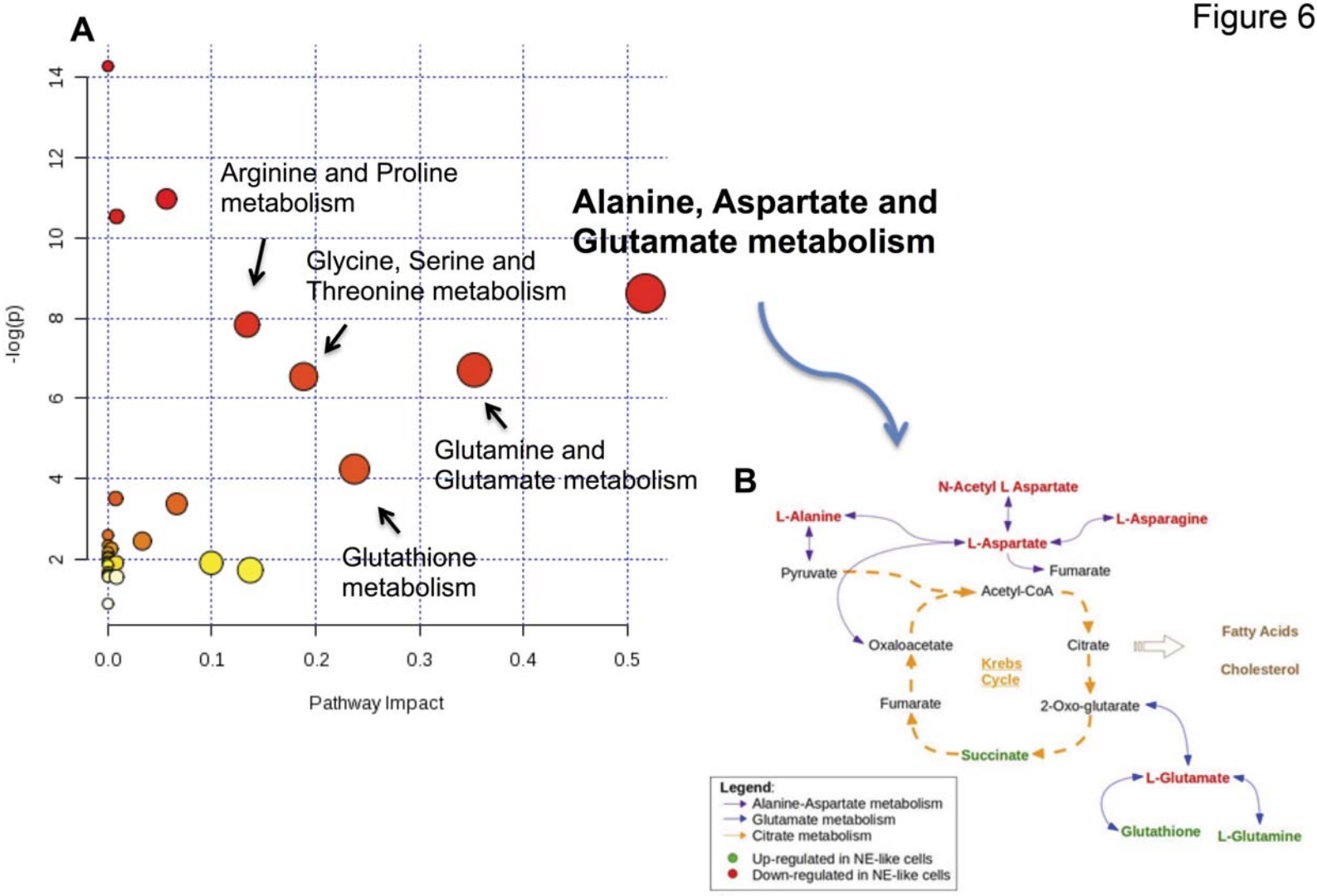

Author Manuscript Published OnlineFirst on June 11, 2015; DOI: 10.1158/0008-5472.CAN-14-3830
Author manuscripts have been peer reviewed and accepted for publication but have not yet been edited.

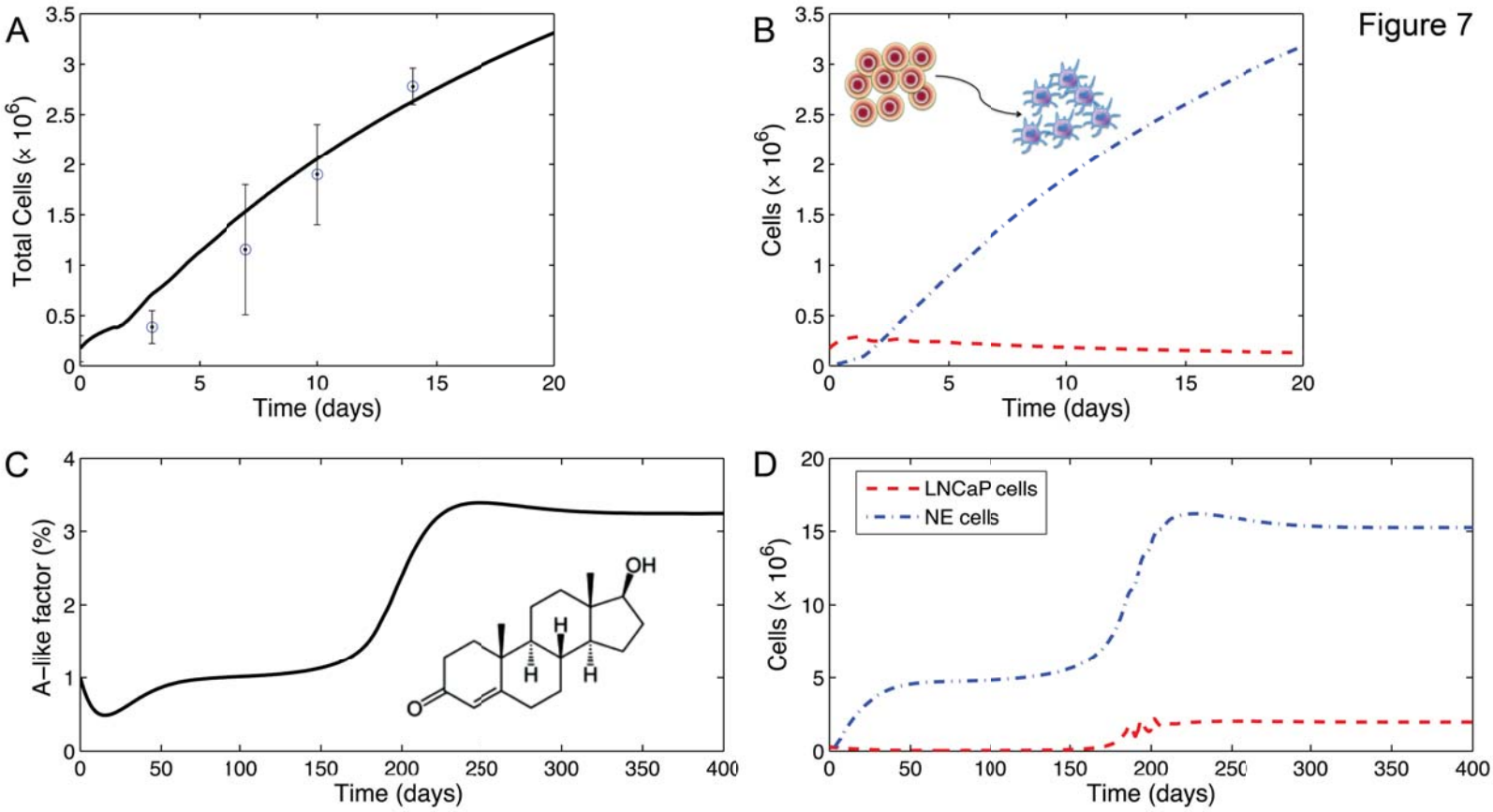


Figure 7

Cancer Research
The Journal of Cancer Research (1916–1930) | The American Journal of Cancer (1931–1940)

AACR American Association for Cancer Research

# Neuroendocrine Transdifferentiation in Human Prostate Cancer Cells: An Integrated Approach

Marianna Cerasuolo, Debora Paris, Fabio Arturo Iannotti, et al.

*Cancer Res* Published OnlineFirst June 11, 2015.